Desalination and Water Treatment
www.deswater.com

doi: 10.5004/dwt.2020.26380

207 (2020) 20–29
December

Superhydrophilic modification of APA-TFC membrane surface for synchronously achieving durable chlorine resistance and high anti-biofouling properties

Bian Hua Fan[a], Jia Jia Wang[b], Yi Zhong Zheng[a], Tian Lin Zhang[a,*]

[a]*Marine Functional Materials Laboratory, School of Chemical Engineering and Materials, Jiangsu Ocean University, Lianyungang 222005, China, email: ldm654123@163.com (T.L. Zhang)*
[b]*Department of Chemical Engineering, Changzhi University, Changzhi 046000, China*

Received 19 February 2020; Accepted 21 July 2020

ABSTRACT

A facile modification method of the aromatic polyamide (APA) thin-film composite (TFC) membrane consisted of two steps. First, the amide N–H group of the aromatic polyamides layer reacted with toluene diisocyanate, which not only eliminated some chlorine-sensitive sites but also left behind the unreacted NCO group on the nascent APA-TFC membrane (referred as to N-membrane) surface. Then, chloride N-(3-formyl-4-hydroxybenzyl)-N,N-dimethyl ammonium-terminated polyethylene glycol (QACs-PEG) was used as the multifunctional alcohol to have an addition reaction with the unreacted NCO group and esterification with the residual acyl chloride group on N-membrane surface. PEG chain terminated with quaternary ammonium cation and salicylaldehyde unit (QACs) was anchored on the APA-TFC membrane surface by these two reactions, and the renascent amide N–H group of carbamide also appeared at the same time. The test results of the modified membrane (M-membrane) performances revealed: (1) due to the abundance of the grafted hydrophilic groups (such as PEG chains and QACs), the surface was superhydrophilic. (2) Compared with the hydrolyzed membrane (H-membrane, prepared from the hydrolysis of N-membrane), the water fluxes of M-membranes significantly increased by nearly 40%. (3) The N–H group of the newly formed urethane was used as a sacrificial unit, which can prevent the aromatic polyamide layer from being corroded by 7×10^5 ppm h chlorine attacking at room temperature. (4) During incubation in the living bacterial suspension, adhesion and growth of gram-negative bacteria *Escherichia coli* and gram-positive bacteria *Staphylococcus aureus* on M-membrane surfaces had been effectively mitigated, which was due to the combination of the steric repulsion of the water-wetting hydration layer and the synergetic contact-killing capabilities of QACs.

Keywords: Supehydrophilic surface modification; Quaternary ammonium cation; Salicylaldehyde; Aromatic polyamide thin-film composite membrane; N,N-Dimethylamino poly(ethylene glycol)

1. Introduction

Today the aromatic polyamide (APA) thin-film composite (TFC) membranes are widely used in the seawater desalination technology because of its simple preparation process [1,2]. The required performances include high hydrophilic surface, high water flux, and high solute rejection, which are seriously affected by biofouling formed by the marine organisms adhering and growing on the membrane surface [3,4]. There are many strategies to control biofouling, such as pretreatment of influent seawater with chlorine of, adding a certain amount of fungicide to the influent seawater, or periodic chemical and physical cleaning of the existing

* Corresponding author.

membranes [5–9]. Among them, chlorine pretreatment is a standard method for controlling biofouling during seawater desalination [10]. However, the aromatic polyamides layer of the APA-TFC membrane is very susceptible to the residual free chlorine disinfectant in the feeding seawater. The chlorination of amide N–H groups of the aromatic polyamides layer of free chlorine leads to the chemical degradation of APA-TFC membranes, resulting in increased water flux and the reduced salt rejection [11–14]. Therefore, the current operational attempts mainly focus on modifying the membrane surface to enhance chlorine resistance [15–18].

Surface modifications by physical coating or chemical grafting with the highly hydrophilic polymers (for example polyethylene glycol (PEG), polyethylene oxide, poly(methacrylic acid)), zwitterionic monomers (such as carboxybetaine, sulfobetaine and phosphorylcholine), and biocides (including triclosan and halamine) were considered to be the potential methods to prepare the membrane which has high hydrophilicity, high anti-biofouling properties or high chlorine-resistance [19,20]. Among the various materials used for grafting, PEG is known for its high resistance to bacterial adhesion. The steric exclusion of the surface hydration layer is considered to be the key to achieve resistance to marine organisms adhering [21–24]. In addition, many reports have confirmed that removing the vulnerable active sites (that is, the amide N–H groups of the aromatic polyamides layer) is an effective method to improve the chlorine resistance of the membranes [25,26].

Inspired by the above-mentioned promising reports, the residual acyl chloride groups on the nascent APA-TFC membrane (abbreviated as N-membrane) were converted into the tertiary amino groups with N,N-dimethylethanolamine and then had the quaternarization with 5-chloromethylsalicylaldehyde. Therefore, in our previous work, the membrane surface was modified in the monomolecular layer with quaternary ammonium cations and salicylaldehyde units (abbreviated as QACs) [27]. In another research, QACs were tightly grafted to the surface of the N-membrane through the amidation of the residual acyl chloride groups [28]. We found that QACs, which are hydrophilic moieties and bactericides, makes the membrane highly hydrophilic and highly resistant to biofouling. Salicylaldehyde units enhanced chlorine resistance by serving as the sacrificial materials. However, the number of the residual acyl chloride groups remaining on the surface of N-membrane is limited, which limits its improvement in hydrophilicity and resistance to chlorine and biofouling.

A facile method was presented to modify the surface of the APA-TFC membrane to synchronously improve the overall performances in this paper as shown in Fig. 1. The first step was the addition reactions of toluene diisocyanate with amide N–H groups of the aromatic polyamides layer on the N-membrane surface, which eliminated some vulnerable sites to free chlorine and leftover the unreacted NCO groups on the surface. Then, chloride N-(3-formyl-4-hydroxybenzyl)-N,N-dimethyl ammonium-terminated polyethylene glycol (QACs-PEG, subdivided into QACs-PEG$_{-1}$, QACs-PEG$_{-3}$ and QACs-PEG$_{-20}$, corresponding to compounds the different PEG chains with the different lengths) was used as the multifunctional alcohol to perform addition reactions with the unreacted NCO groups and esterifications with the acyl chloride groups. The PEG chains and QACs were anchored on the surface, and the nascent amide N–H groups of carbamides appeared simultaneously.

2. Experimental section

2.1. Materials and reagents

The commercial APA-TFC reverse osmosis membrane (referred to as C-membrane as a reference) was offered by the Development Center of Water Treatment Technology (Hangzhou, China) with a typical salt rejection of 98.3% and the water flux of 60.0 L/m^2 h for a feedwater solution containing 2,000 mg/L NaCl at 1.0 MPa. Toluene diisocyanate (TDI), di-*n*-butyltin dilaurate (DBTDL), triethylene amine (TEA), cyclohexane, dioxane and N,N-dimethylaminoethanol (DMAPEG$_{-1}$) were purchased from Jingchun Chemical Reagent Co., Ltd., (Shanghai, China), and used without further purification. N,N-dimethylamino triglycol (DMAPEG$_{-3}$) and ω-dimethyl amino poly(ethylene glycol)-1000 (DMAPEG$_{-20}$) was prepared according to the literature [29]. 5-chloromethylsalicylaldehyde was prepared according to the literature [30]. Sodium hypochlorite solution (NaClO, 5.1 wt.%) used as the chlorine aqueous solution in the membrane chlorination test was purchased from Family Happy Supermarket (Lianyungang, China).

2.2. Preparation process of the modified APA-TFC membrane

DMAPEG$_{-1}$, DMAPEG$_{-3}$ or DMAPEG$_{-20}$ were dissolved into toluene solution, and cyclohexane solution containing 5-chloromethylsalicylaldehyde was added. The mixture was stirred for 6 h at room temperature. The precipitate of QACs-PEG (which is QACs-PEG$_{-1}$, QACs-PEG$_{-3}$ or

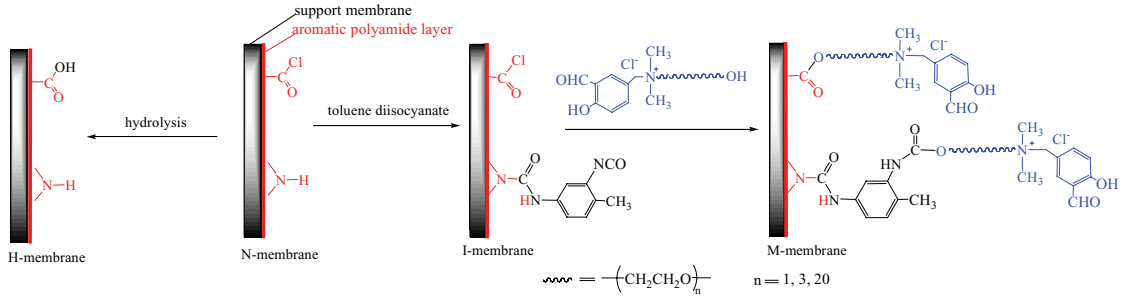

Fig. 1. Schematic illustration of the modified APA-TFC membrane.

QACs-PEG$_{-20}$, respectively) was separated from the toluene solution and washed with toluene and dissolved into dioxane for standby.

N-membrane, which was fabricated via the interfacial polymerization of *m*-phenylenediamine and trimesoyl chloride on the porous polysulfone support membrane according to the reported method [22,27], and was immersed in dioxane solution containing TDI (0.5, 5.0 or 10.0 wt.%) and DBTDL (0.3 wt.%) as the catalyst at 60°C under nitrogen atmosphere for 6 h, and washed with dioxane to remove the unreacted TDI. And then the membrane (I-membrane) containing acyl chloride groups and NCO groups on its surface were soon immersed in dioxane solution containing QACs-PEG$_{-1}$, QACs-PEG$_{-3}$ or QACs-PEG$_{-20}$ (0.5, 5.0 or 10 wt.%) and TEA (10 wt.%) and DBTDL (0.5 wt.%) at 60°C–65°C for 12 h, and washed with ethanol and water to remove the unreacted QAC-PEG, thus the modified APA-TFC membrane (referred to as M-membrane, subdivided into M-membrane$_{-1}$, M-membrane$_{-3}$ or M-membrane$_{-20}$, respectively) with PEG chains and QACs on the surface were successfully prepared.

2.3. Membrane characteristics

2.3.1. Spectral analysis and physical characterization

The structural changes of the membrane surface were monitored during the modification process by using MAGNA-560 AT (USA) attenuated total reflectance-Fourier-transform infrared spectroscopy (ATR-FTIR). Before testing, the membrane samples including N-membrane, H-membrane (which was prepared from N-membrane after hydrolysis), and M-membranes were dried at 40°C. In order to characterize hydrophilicity, the water contact angle (WCA) of the membrane surfaces were measured using a sessile drop method with a contact angle analyzer using OCA15EC Dataphysics (Germany). The pure water was used as the probe liquid. Prior to the measurements, all membrane samples were conditioned at 40°C under 50% relative humidity for 24 h. At least three stabilized contact angles from different sites of each sample were obtained to calculate the average contact angle [31]. According to the previous report [32], the tangential streaming potential (ΔE) of the membrane surface was measured in 0.01 M potassium chloride aqueous solution at different pH. ΔE was measured at five different pressures (ΔP) ranging from 0.1 to 0.5 bar. The zeta potential (ξ) was calculated by the classic Helmholtz–Smoluchowski Eq. (1).

$$\xi = \frac{\Delta E \cdot \mu \cdot \eta}{\Delta P \cdot \varepsilon} \tag{1}$$

where ε is the dielectric constant, and μ and η are the viscosity and conductivity of the solution, respectively.

Scanning electron microscopy (SEM) of the membrane surface was carried out using a field-emission scanning electron microscopy (FE-SEM) Hitachi S-4800 (Japan). Quantitative surface roughness analysis of the membrane was measured using an atomic force microscope (AFM, Park Systems XEI-100E, Korea) imaging and analysis in the tapping mode. The root means square roughness was used to compare the surface roughness.

2.4. Evaluation of membrane anti-biofouling abilities

Mainly investigated the chlorine resistance and anti-biofouling properties of the modified membranes, and compared them with C-membrane and H-membrane. According to the reported procedure [33,34], the accelerated chlorination test was conducted to evaluate the chlorination resistance of the membrane samples. The procedure of the accelerated chlorination test was to soak the membrane samples in an aqueous solution of sodium hypochlorite with an effective chlorine concentration of 7,000 ppm at pH 7.0 for 20–100 h at room temperature. The water fluxes (F_w) and the salt rejections (R) of the membrane samples before and after the chlorination treatment was measured in terms of a liter per square meter per hour (L/m^2 h) using 2,000 ppm NaCl aqueous solution under 1.0 MPa at 25°C and at pH 7.0, and calculated from Eqs. (2) and (3).

$$F_w = \frac{\Delta V}{A \cdot \Delta t} \tag{2}$$

where A is the effective membrane area (m^2), and ΔV is a permeating volume (L), Δt is the permeating time (h).

$$R = \frac{C_f - C_p}{C_f} \times 100\% \tag{3}$$

where C_f and C_p are the salt concentrations in the feed and permeate solutions, respectively, and determined by measuring the electrical conductance using a conductance meter (DDSJ-308A, Cany Precision Instruments Co., Ltd., China).

Advocating the enhancement of the anti-bioadhesion ability and the capability to endow the contact-killing are the two main strategies for improving the anti-biofouling of the membrane surface [35,36]. Gram-negative bacteria *Escherichia coli* (*E. coli*) and gram-positive bacteria *Staphylococcus aureus* (*S. aureus*) were used as the model microorganisms to test the anti-biofouling properties of the membrane samples. A diluted bacterial suspension at proximately 1.0 × 10^6 colony-forming units per milliliter (CFU mL^{-1}) concentration was dispensed onto the membrane (2.5 cm diameter), and an inoculum containing 1 wt.% bacto tryptone, 0.5 wt.% yeast extract, and 0.1 wt.% NaCl was added to the suspension. After incubating at 37°C for 24 h, the contaminated was gently rinsed with water to remove the unattached bacteria and then evaluated for bacterial adhesion and contact-killing by the fluorescence microscope. The static water fluxes and salt rejections of the membrane samples were measured using 2,000 ppm NaCl aqueous solution before and after the pollution under 1.0 MPa at 25°C. According to the reported procedure [37], the diluted living bacteria suspension was added into the feed NaCl aqueous solution at 1 mL/1 L once every 4 h.

3. Results and discussion

3.1. Preparation of M-membranes

The amide N–H groups of the aromatic polyamides layer are known to be sensitive sites to chlorine disinfectants, however, they can also have the addition reaction with TDI

on the APA-TFC membrane surface [38,39]. Therefore, in the experiment, one of two NCO groups in TDI used as the linking reagent was subjected to an addition reaction with amide N–H group of the aromatic polyamides layer. The aim is to eliminate some of the vulnerable sites to free chlorine. Another unreacted NCO group temporarily remained on the membrane surface. The reaction results of TDI on the surface of the N-membrane was expressed in term of the content of the unreacted NCO groups, which was determined by the back titration with di-*n*-butylamine [40], as shown in Fig. 2.

When the concentration of TDI was lower in dioxane solution, there were no enough TDI molecules to react with amide N–H groups of the aromatic polyamides, and the fewer NCO groups were anchored on the membrane surface. As the TDI concentrations in dioxane solution increased during the reaction, the content of the unreacted NCO groups increased distinctly on the surface. Meanwhile, with the extension of the reaction time, NCO content would also be increased on the surface. When the concentration of TDI was 10 wt.% in dioxane solution, NCO content on the N-membrane surface increased almost linearly with the reaction time. This might mean that when amide N–H groups on the surface of the aromatic polyamides layer was exhausted, the addition reactions did not end. The excessive free TDI would react further with the nascent carbamate N–H group, leaving behind another unreacted NCO group, so the content of the unreacted NCO group will increase with the increase of reaction time, as shown in Fig. 3.

The above phenomenon showed that the content level of the unreacted NCO group on the surface was closely related to the concentration of TDI in dioxane solution and the reaction time, which might influence the permeation and filtration performances of the subsequent M-membranes. Therefore, in order to select the appropriate NCO content on the surface, the permeation and filtration performances of I-membranes were indirectly tested after treating with di-*n*-butylamine to optimized the reaction time and temperature and the concentration of TDI in dioxane solution. The tested results are shown in Figs. 4 and 5.

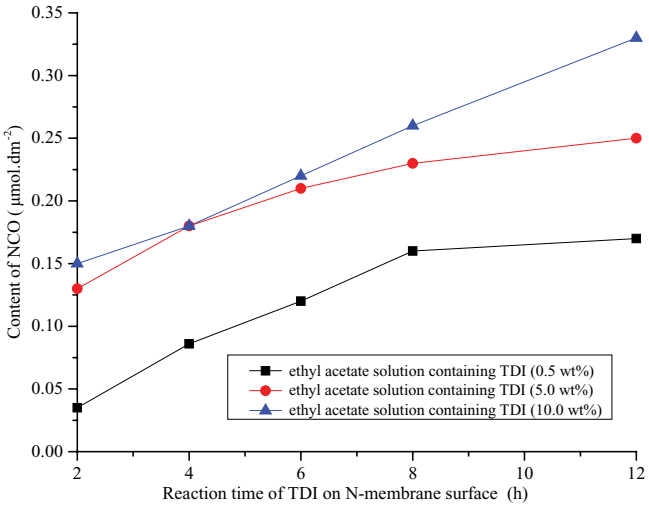

Fig. 2. Content of NCO remaining on the membrane surface at different reaction times.

The water flux of D-membrane produced from N-membrane treated with di-*n*-butylamine was 43.4 L/m^{-2} h, which was about 8% smaller than 47.2 L/m^{-2} h for H-membrane [27]. H-membrane is similar to the commercial APA-TFC membrane (C-membrane), and its desalination was 99.1%, which is 0.3% lower than 99.4% of D-membrane. Compared with the H-membrane, the water flux of D-membrane was reduced, which was due to the reduced hydrophilicity of its surface. When the reaction temperature was between 20°C–50°C, the reaction rate of TDI with amide N–H groups was very small within the reaction period of 6 h. No fluctuation was observed in the water permeation and salt filtration of DD-membranes. When the temperature was above 60°C, TDI worked quickly. With the transformation of the amide N–H groups into the carbamides groups and the interchain hydrogen bonds of the aromatic polyamides layer was partially broken. The passing rate of DD-membrane in both water and salt was obviously increased. This was the similar results obtained by chlorination of the amide N–H groups of the aromatic polyamides layer [41,42]. When the temperature rising to 100°C, TDI would be penetrated into the interior of the aromatic polyamides layer to take the reactions with the more amide N–H groups, resulting in the more losses of the interchain hydrogen bonds, and the stronger mobility and conformational alteration of the aromatic polyamide chains. Therefore, as shown in Fig. 4, a sharp increase in water flux and a significant decrease in the desalination rate were observed. Taken together, to ensure the enough NCO content on the membrane surface, and to inhibit the excessive consumption of the inter-chain hydrogen bonds in the aromatic polyamide layer, the suitable reaction temperature was selected at 60°C, the reaction time was 6 h, and the concentration of TDI in dioxane was 5 wt.%.

After the reaction of I-membrane with QACs-PEG, the modified membranes (abbreviated as M-membranes, subdivided as to M-membrane$_{-1}$, M-membrane$_{-3}$, M-membrane$_{-20}$, respectively) were finally prepared. As shown in Fig. 6, the densities of QACs anchored on the surfaces of M-membrane was calculated based on the potential titration analysis of $AgNO_3$ chloride anions. It could be seen that the higher length of the PEG chain in QACs-PEG, the lower reactivity of QACs-PEG, and the lower density of QACs on M-membrane surfaces. However, it was important that QACs densities on M-membranes were much higher than the results in our previous works [27,28]. This indicated that TDI-based modification of the membrane surface showed an advantage in grafting a higher density of QACs.

3.2. Spectral and morphology analysis

Throughout the modification process, the structural changes of the APA-TFC membrane surface were confirmed by ATR-FTIR. In Fig. 7, the characteristic adsorption bands of N-membrane appeared at 1,767; 1,665 and 1,608 cm^{-1} in the IR spectrum, which corresponded to the residual acyl chloride C=O, polyamide C=O stretching, and benzene-ring C=C stretching, respectively. After reacting with TDI, the IR spectrum of I-membrane showed the characteristic adsorption bands at 1,638; 1,733 and 2,270 cm^{-1}, corresponding to the carbamide units (–NHCOO–), (–NHCONH–) and phenyl isocyanate (ph-NCO) units, respectively. After the reactions

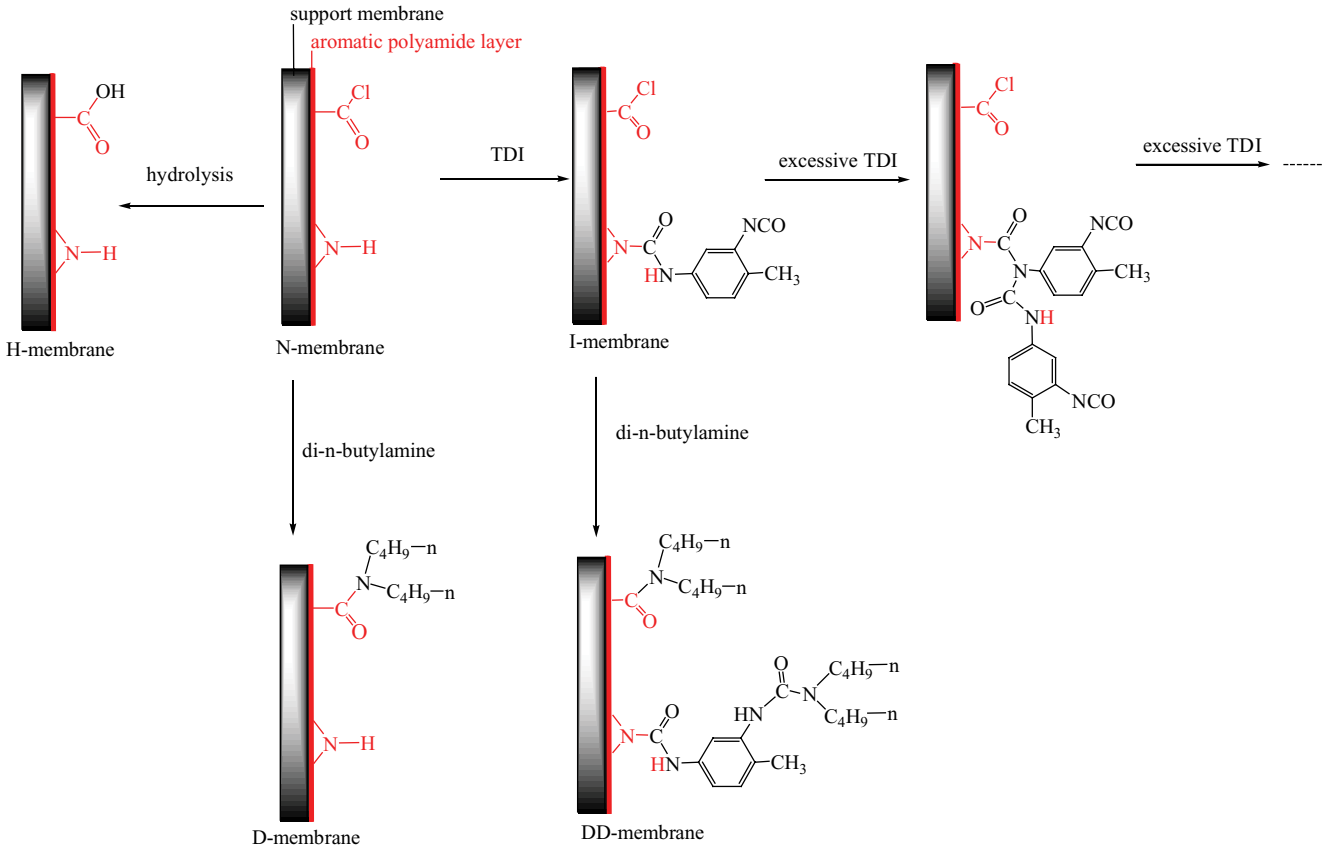

Fig. 3. Preparation processes of H-membrane, I-membrane, D-membrane and DD-membrane.

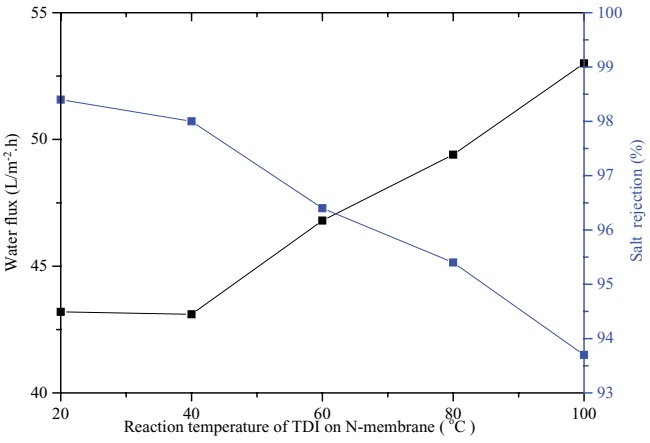

Fig. 4. Permeation and filtration performance of DD-membranes. The concentration of TDI in the dioxane solution was 5 wt.%. The reaction time was set at 6 h.

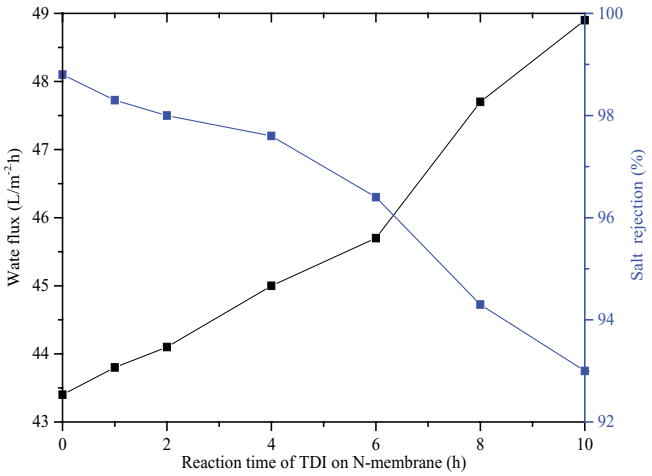

Fig. 5. Performances of DD-membranes. The concentration of TDI was 5 wt.% in dioxane solution, the reaction temperature was set at 60°C.

of I-membrane with QACs-PEG$_{-1}$, the peak at 1,767 cm^{-1} decreased significantly, and the medium intensity peak belonged to the renascent ester C=O stretching appeared at 1,726 cm^{-1} in the spectrum of M-membrane$_{-1}$. The results of the $AgNO_3$ titration analysis of the chloride anion and the characteristic adsorption bands in FTIR both proved that the preparation of M-membrane$_{-1}$ was successful.

The surface morphology images of the membrane samples including H-membrane and M-membranes were recorded by FE-SEM Hitachi S-4800 (Japan) and AFM Park Systems XEI-100E (Korea). In Fig. 8, these photos exhibit that all of the tested membrane surfaces are the typical peak-and-valley morphology. The H-membrane surface

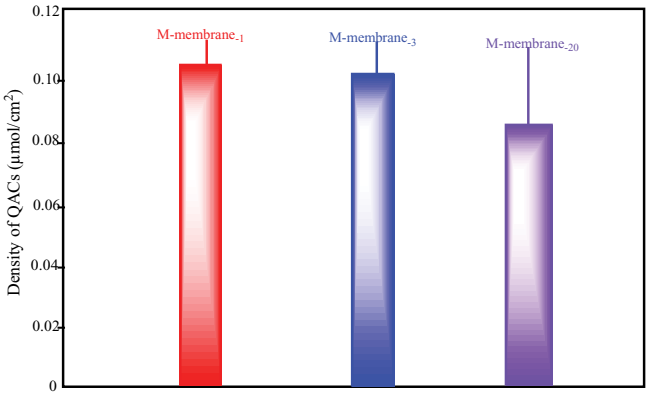

Fig. 6. The density of quaternary ammonium cations on M-membrane surfaces.

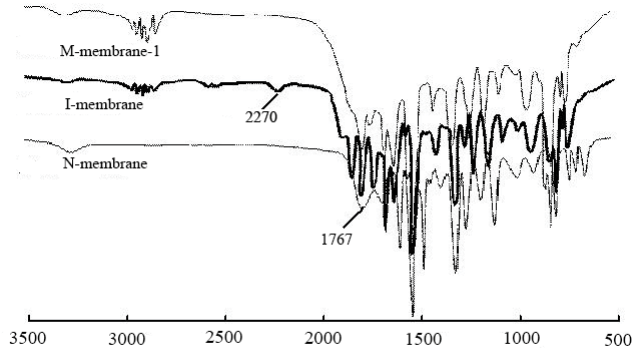

Fig. 7. FTIR spectra of membrane samples (cm^{-1}).

is relatively loose. After the modifications, M-membrane surfaces became denser with increasing the grafted QACs. Meanwhile, it could be clearly seen that M-membrane$_{-20}$, M-membrane$_{-3}$ and M-membrane$_{-1}$ were roughened with the more slender ridges than H-membrane. The root mean square roughness values, such as 96.9, 107.6, 124.2 and 126.3 nm corresponding to H-membrane, M-membrane$_{-1}$, M-membrane$_{-3}$ and M-membrane$_{-20}$, respectively, indicated a tendency of the surface roughness increase with increasing the length of PEG chains.

3.3. Physical characteristics of membranes

Both of H-membrane and C-membrane have carboxylic acid groups on their surfaces. Therefore, as shown in Fig. 9, at pH above 5.5, their zeta potentials were below zero, which was due to the dissociation of carboxylic acid groups. Due to quaternary ammonium cations, all three M-membranes showed a positive zeta potential at pH 3~10. In addition, among these three M-membranes, because of the highest density of quaternary ammonium cations on its surface, M-membrane$_{-1}$ showed the highest zeta potential. The positive zeta potentials of all three M-membranes decreased sharply as pH increased from 9 to 10, resulting from the deprotonation of phenol groups in salicylaldehyde units in the strong alkaline solution.

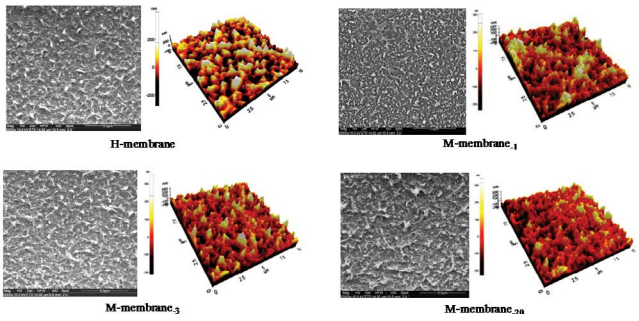

Fig. 8. Surfaces SEM and AFM images of the membrane samples.

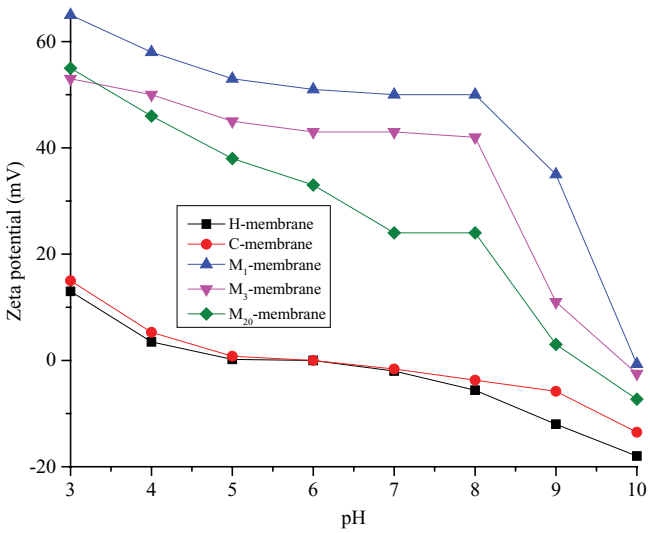

Fig. 9. Zeta potential of membrane samples at different pH.

WCA of C-membrane was measured to be 57° ± 0.8°, agreeing with the technical parameter (58° ± 0.5°) from the membrane supplier, and the WCA of H-membrane was 54° ± 1.3° about 3° smaller than C-membrane. The contact angles of all three M-membranes dropped to 0°, which demonstrated that M-membrane surfaces were superhydrophilic in favor of binding the water molecules and generating a tight hydration layer [43,44]. This demonstrated that TDI-based surface modification is a facile method for preparing the super-hydrophilicity desalination membrane.

3.4. Anti-biofouling properties

The anti-biofouling performances were examined by cultivating the membrane samples in the living suspension containing *E. coli* or *S. aureus* for 24 h at 37°C. The adhering, growing and death situation of bacteria on the membrane surfaces were shown by the fluorescence microscope images as shown in Fig. 10. The living bacteria were stained by SYTO9 and showed in green, and the dead bacteria were stained by propidium iodide and showed in red.

In Fig. 10, the green fluorescence microscope photos showed that *E. coli* adhered to the carboxylate membranes and grew well. This suggested that both of C-membrane and H-membrane all lacked resistance to the bacterial adhesion.

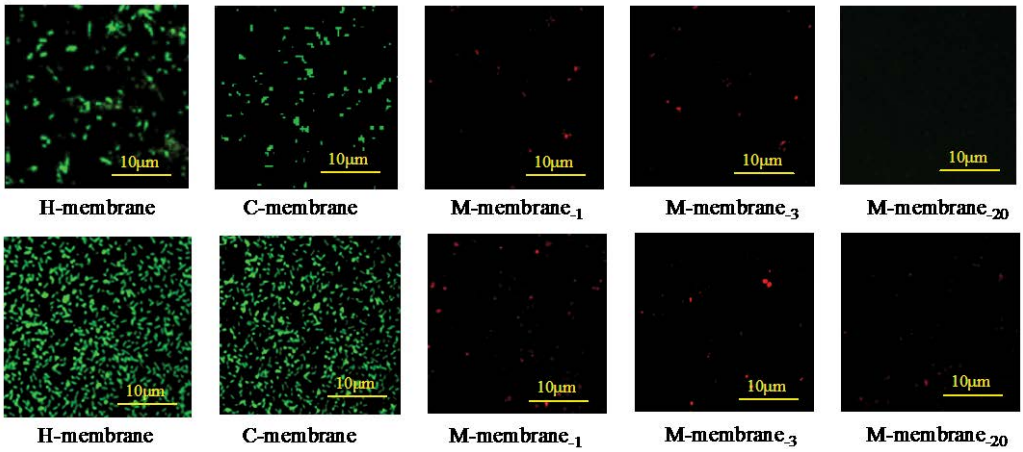

Fig. 10. Fluorescence microscope images of *E. coli* (up) and *S. aureus* (down) living adhered, growing and died on the membrane surfaces.

In contrast, almost all bacteria attached to the surfaces of M-membrane died. This revealed that M-membranes had a strong contact-killing ability to *E. coli* bacteria, which was due to the synergistic disinfection from QACs and salicylaldehyde units. In addition, no dead bacteria adhesion observation was made on the surface of the M-membrane$_{-20,}$ indicating that PEG reduced bacteria adhesion. In general, the hydrophilic PEG chains enhanced the resistance to bacterial adhesion, and QACs exhibited strong contact-killing capability. Furthermore, the living adhesion and growth density of *S. aureus* bacteria on C-membrane and H-membrane surfaces was higher than that of *E. coli*. *S. aureus* bacteria on M-membranes almost entirely dead, similar to *E. coli*. The above experiment results showed that the higher density of QACs and PEG chains on the M-membrane surface, the strong bacterial contact-killing capacity and the higher adhesion resistance to *E. coli* and *S. aureus* bacteria.

The dynamic simulation experiment on the biofouling permeation was performed on a laboratory scale. Before conducting the anti-biofouling test, the original membrane samples were first permeated to get a constant flux value as the references using 2,000 ppm NaCl aqueous solution under 1.0 MPa at pH 7.0 and 25°C for the first 8 h. Then the diluted *E. coli* suspension was added into NaCl aqueous solution in a ratio of 1 mL/L once every 4 h. Under the same conditions, the water fluxes were monitored over 16 h. The water flux changes were listed in Table 1 for each membrane over time. The water flux changes were expressed by the water flux decline percentage (D). It could be calculated from Eq. (4):

$$D = \frac{V - V_1}{V_1} \times 100\% \tag{4}$$

In Eq. (4), D was the declining percentage of the water flux, V was the permeate water value at a given time period, and V_1 was the permeate water value during the first-hour permeation filtration.

It could be seen from Table 1 that the water flux of all membrane samples remained relatively constant during the first 8 h of filtration period before fouling occurred. All of the modified membranes displayed the higher water fluxes than H-membrane, which confirmed the previous result that improving the hydrophilicity of the membrane surface was a benefit to enhance the water flux [45,46]. After adding the diluted *E. coli* suspension to the feed NaCl aqueous solution, the water fluxes of all membrane samples decreased in varying degrees as the filtration continued. The water fluxes of C-membrane and H-membrane were 56% and 53.6% of their initial values after 24 h permeation filtration, respectively. But the water flux decreases of M-membrane$_{-1}$, M-membrane$_{-3}$ and M-membrane$_{-20}$ were 20.3%, 18.2% and 6.2% respectively, as shown in Fig. 11.

Table 1
Water fluxes of membranes in dynamic simulate biofouling experiment

Permeation time (h)							
Water flux (L/m^2 h)	1	4	8	12	16	20	24
Membrane samples							
C-membrane	59.7	60.0	60.0	54.3	49.6	36.9	26.2
H-membrane	47.2	47.2	47.4	43.2	41.7	30.7	21.9
M-membrane$_{-1}$	66.3	66.5	66.5	62.7	60.5	57.7	52.8
M-membrane$_{-3}$	66.4	66.5	66.5	65.1	64.0	59.2	54.3
M-membrane$_{-20}$	65.9	65.9	65.9	64.3	63.8	62.3	61.8

It is naturally supposed that the positively charged M-membranes should attract a large number of bacteria with the negative charges to adhere to the surfaces by the electrostatic interaction, forming the biofouling, and resulting in sharp decline of the water fluxes. However, M-membranes showed a lower percentage of water fluxes than the carboxylate membranes. This was due to PEG and QACs on M-membranes had a strong contact-killing capacity, which can prevent bacterial adhesion and growth. In particular, M-membrane$_{-20}$ retained the more than 93% of its initial water flux value during the range of 24 h permeation filtration. This also indicated that the PEG hydration layer is indispensable to prevent bacteria from adhering to and growing on the surface.

The salt rejections of the polluted M-membranes were generally smaller than that of the carboxylate membranes as shown in Fig. 12. This might be because grafting of QACs on M-membranes led to some breakdown of the interchain hydrogen bonds of the aromatic polyamides layer, which increased the chain mobility and caused the conformational alteration of the aromatic polyamides chains [13,47,48]. The increase in the number of QACs led to an increase in the passage of water and salt. Therefore, the interchain hydrogen bonds in the aromatic polyamide layer play an important role in the salt rejection of APA-TFC membranes.

3.5. Evaluation of chlorine resistance

The water fluxes and salt rejections of the chlorinated membrane samples were evaluated by filtration using 2,000 ppm NaCl aqueous solution under 1.0 MPa at 25°C and at pH 7.0, as seen as Figs. 13 and 14. Because amide N–H groups of the aromatic polyamide layer on the carboxylate membrane surfaces were chlorinated to form N–Cl groups after treatment in the aqueous solution containing 7,000 mg L^{-1} free chlorine at pH 7.0 for 20–100 h at room temperature. This led to the various degrees of damage to the pristine structure for the aromatic polyamide layer, which enhanced the peristalsis and mobility of the aromatic polyamide chains. Therefore, the increase of water and salt passages for the chlorinated carboxylate membranes were observed. Meanwhile, the increment of the water fluxes did not decrease for the carboxylate membranes with increasing chlorination time in 7,000 ppm chlorine aqueous solution during the testing. This indicated there were no protections for the carboxylate membranes. The water fluxes of H-membrane and C-membrane increased by 23.8% and 20.5%, while the desalination rate decreased by 4.7% and 5.6% after 7 × 10^5 ppm h chlorination, respectively. However, under the same chlorination conditions, the water fluxes of all the chlorinated M-membranes exhibited slight changes in all the permeation test. After 7,000 × 100 ppm h chlorination reaction, the water fluxes of M-membrane$_{-1}$, M-membrane$_{-3}$ and M-membrane$_{-20}$ increased by 8.6%, 12.6% and 12.3%, and their salt rejections decreased by 0.8%, 1.3% and 1.1%, respectively. This indicated that M-membranes had high stability in the chlorine aqueous solution. We proposed two hypotheses to explain the phenomenon. Firstly, salicylaldehyde units as the sacrificial materials preferentially reacted with the free chlorine to protect the aromatic polyamide layers of the modified membranes. The higher salicylaldehyde density anchored on the modified membrane surfaces, the higher resistance to the free chlorine attacking. Secondly, the renascent carbamides, which appeared at the same time when anchoring QACs on the modified membrane surface, have the electron-donating methyl groups adjacent to amide N–H groups and show the higher reactivity with free chlorine than amides N–H groups of the aromatic polyamide layers. Therefore, the renascent amide N–H groups of carbamides can also be used as the sacrificial pendant groups to protect the modified membranes suffered from the free chlorine attacking [49,50]. To sum up, based on QACs serving as the highly hydrophilic groups and the strong bactericides, and PEG chains forming the tight hydration layer, and salicylaldehyde units and carbamides serving as the sacrificial materials, the overall performances of the modified APA-TFC membrane were simultaneously improved.

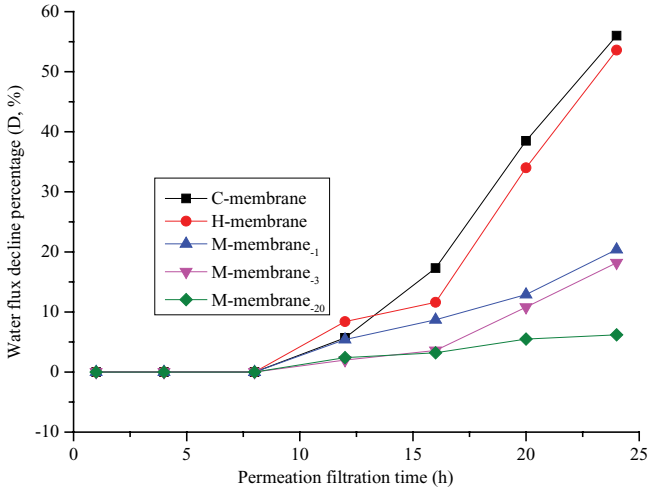

Fig. 11. Water fluxes of pollution membranes during the permeation filtration.

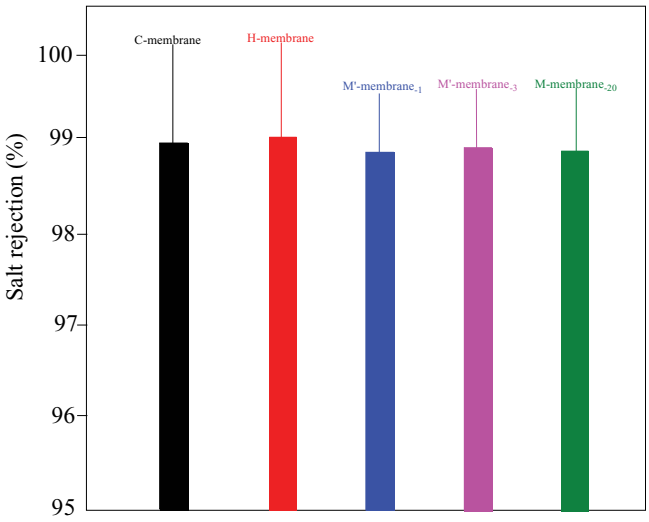

Fig. 12. Salt rejection of the polluted membranes during the permeation filtration.

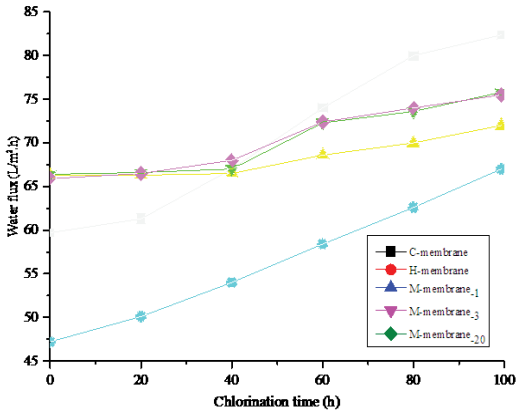

Fig. 13. Water fluxes of the chlorinated membranes in 7,000 ppm chlorine aqueous solution at room temperature.

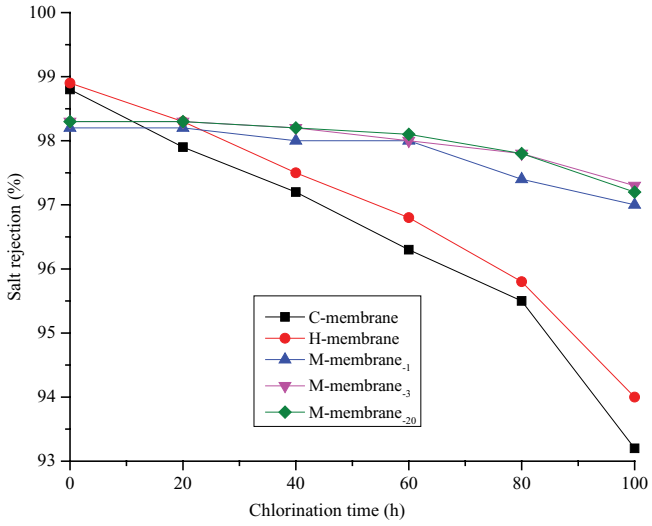

Fig. 14. Salt rejection of the membranes after chlorination in 7,000 ppm chlorine solution.

4. Conclusion

By using polyethylene glycol as a spacer in this work, quaternary ammonium cation and salicylaldehyde units and TDI were densely grafted onto the surface of the monomolecular layer APA-TFC membrane. The chemical compositions of the modified membrane surfaces were determined by instrumental analysis and chemical analysis. The WCAs of the modified membranes dropped to 0°. All of the three M-membranes showed the positive zeta potentials at pH 3~8. During the permeation filtration tests, the modified membrane showed highly chemical stability in the chlorination under the condition of 7×10^5 ppm h. The high grafting density of QACs on the modified membranes showed positive effects on the water fluxes and the slightly negative effect on salt rejection. The long-chain poly(ethylene glycol) formed a hydration layer to significantly reduce the adhesion of *E. coli* or *S. aureus* on the modified membrane surfaces, and QACs endowed the modified membranes with the strong contact-killing capacities. In a word, the super-hydrophilic APA-TFC membrane with PEG chains, the surface QACs presented high water flux, high anti-biofouling and excellent resistance to the free chlorine, which in the desalination technology has great potential.

Acknowledgments

This work was supported by the Natural Science Foundation of Jiangsu Province (BK20161294), Lian Yun Gang Science Project (CG1602), Natural Science Foundation of Jiangsu Province (BK20160434), and University Science Research Project of Jiangsu Province (15KJB430004). There is no conflict of interest between funding agencies.

References

[1] M. Elimelech, W.A. Phillip, The future of seawater desalination: energy, technology, and the environment, Science, 333 (2011) 712–719.
[2] M. Asadollahi, D. Bastani, S.A. Musavi, Enhancement of surface properties and performance of reverse osmosis membranes after surface modification: a review, Desalination, 420 (2017) 330–383.
[3] A. Matin, Z.K. Han, S.M.J. Zaidi, M.C. Boyce, Biofouling in reverse osmosis membranes for seawater desalination: phenomena and prevention, Desalination, 281 (2011) 1–16.
[4] N. Misdan, A.F. Ismail, N. Hilal, Recent advances in the development of (bio)fouling resistant thin film composite membranes for desalination, Desalination, 380 (2016) 105–111.
[5] D. Kim, S.H. Jung, J. Sohn, H.S. Kim, S.H. Lee, Biocide application for controlling biofouling of SWRO membranes-an overview, Desalination, 238 (2009) 43–52.
[6] M.T. Khan, P.Y. Hong, N. Nada, J.P. Croue, Does chlorination of seawater reverse osmosis membranes control biofouling?, Water Res., 78 (2015) 84–97.
[7] T. Nguyen, F. Roddick, L. Fan, Biofouling of water treatment membranes: a review of the underlying causes, monitoring techniques and control measures, Membranes, 2 (2012) 804–840.
[8] L. Vanysacker, R. Bernshtein, I.F.J. Vankelecom, Effect of chemical cleaning and membrane aging on membrane biofouling using model organisms with increasing complexity, J. Membr. Sci., 457 (2014) 19–28.
[9] S.F. Anisa, R. Hashaikehb, N. Hilal, Reverse osmosis pretreatment technologies and future trends: a comprehensive review, Desalination, 452 (2019) 159–195.
[10] V. Bonnely, M.A. Sanz, J.P. Durand, L. Plasse, F. Gueguen, P. Mazounie, Reverse osmosis on open intake seawater: pretreatment strategy, Desalination, 167 (2004) 191–200.
[11] R. Singh, Polyamide polymer solution behaviour under chlorination conditions, J. Membr. Sci., 88 (1994) 285–287.
[12] G.D. Kang, C.J. Gao, W.D. Chen, X.M. Jie, Y.M. Cao, Q. Yuan, Study on hypochlorite degradation of aromatic polyamide reverse osmosis membrane, J. Membr. Sci., 300 (2007) 165–171.
[13] J. Powell, J. Luh, O. Coronell, Amide link scission in the polyamide active layers of thin-film composite membranes upon exposure to free chlorine: kinetics and mechanisms, Environ. Sci. Technol., 49 (2015) 12136–12144.
[14] J.M. Gohil, A.K. Suresh, Chlorine attack on reverse osmosis membranes: mechanisms and mitigation strategies, J. Membr. Sci., 541 (2017) 108–126.
[15] D. Rana, T. Matsuura, Surface modifications for antifouling membranes, Chem. Rev., 110 (2010) 2448–2471.
[16] R. Verbeke, V. Gómez, F.J. Vankelecom, Chlorine-resistance of reverse osmosis (RO) polyamide membranes, Prog. Polym. Sci., 72 (2017) 1–15.
[17] V. Nagaraj, L. Skillman, D. Li, G. Ho, Review–bacteria and their extracellular polymeric substances causing biofouling on seawater reverse osmosis desalination membranes, J. Environ. Manage., 2231 (2018) 586–599.

[18] A. Matin, F. Rahman, H.Z. Shafi, S.M. Zubair, Scaling of reverse osmosis membranes used in water desalination: phenomena, impact, and control; future directions, Desalination, 4551 (2019) 135–157.
[19] J. Wang, Z. Wang, J.X. Wang, S.C. Wang, Improving the water flux and bio-fouling resistance of reverse osmosis (RO) membrane through surface modification by zwitterionic polymer, J. Membr. Sci., 493 (2015) 188–199.
[20] S.-H. Park, S.O. Hwang, T.-S. Kim, A. Cho, S.J. Kwon, K.T. Kim, H.-D. Park, J.-H. Lee, Triclosan-immobilized polyamide thin film composite membranes with enhanced biofouling resistance, Appl. Surf. Sci., 443 (2018) 458–466.
[21] Y. Zhang, Y. Wan, G.Y. Pan, H.W. Shi, H. Yan, J. Xu, M. Guo, Z. Wang, Y.Q. Liu, Surface modification of polyamide reverse osmosis membrane with sulfonated polyvinyl alcohol for antifouling, Appl. Surf. Sci., 419 (2017) 177–187.
[22] M. Ravindra Gol, S.K. Jewrajka, Facile *in situ* PEGylation of polyamide thin film composite membranes for improving fouling resistance, J. Membr. Sci., 455 (2014) 271–282.
[23] D.J. Miller, P.A. Araújo, P.B. Correia, M.M. Ramsey, J.C. Kruithof, M.C.M. van Loosdrecht, B.D. Freeman, D.R. Paul, M. Whiteley, J.S. Vrouwenvelder, Short-term adhesion and long-term biofouling testing of polydopamine and poly(ethylene glycol) surface modifications of membranes and feed spacers for biofouling control, Water Res., 46 (2012) 3737–3753.
[24] X.Q. Cheng, L. Shao, C.H. Lau, High flux polyethylene glycol based nanofiltration membranes for water environmental remediation, J. Membr. Sci., 476 (2015) 95–104.
[25] T.L. Zhang, K.R. Zhang, J.H. Li, X.D. Yue, Simultaneously enhancing hydrophilicity, chlorine resistance and anti-biofouling of APA-TFC membrane surface by densely grafting quaternary ammonium cations and salicylaldimines, J. Membr. Sci., 528 (2017) 296–302.
[26] S.S. Lin, H. Huang, Y.J. Zeng, L. Zhang, L.A. Hou, Facile surface modification by aldehydes to enhance chlorine resistance of polyamide thin film composite membranes, J. Membr. Sci., 518 (2016) 40–49.
[27] T.L. Zhang, C.Y. Zhu, H.M. Ma, R.Y. Li, B.G. Dong, Y.F. Liu, S.Z. Li, Surface modification of APA-TFC membrane with quaternary ammonium cation and salicylaldehyde to improve performance, J. Membr. Sci., 457 (2014) 88–94.
[28] T.L. Zhang, X.D. Yue, C.Y. Zhu, H.M. Ma, Y.B. Liu, J.N. Li, Densely grafting quaternary ammonium cation and salicylaldehyde on the APA-TFC membrane surface for enhancing chlorine resistance and anti-biofouling properties, Desal. Water Treat., 57 (2016) 1–11.
[29] M. Mutter, Soluble polymers in organic synthesis: I. Preparation of polymer reagents using polyethylene glycol with terminal amino groups as polymeric component, Tetrahdron Lett., 31 (1978) 2839–2842.
[30] T.L. Zhang, J.J. Wang, J.T. Ni, Process of 5-Chloromethyl-salicylaldehyde, CN201110063509, 2011.
[31] Y.F. Mi, Q. Zhao, Y.L. Ji, Q.F. An, C.J. Ga, A novel route for surface zwitterionic functionalization of polyamide nanofiltration membranes with improved performance, J. Membr. Sci., 490 (2015) 311–320.
[32] G. Hurwitz, G.R. Guillen, E.M.V. Hoek, Probing polyamide membrane surface charge, zeta potential, wettability, and hydrophilicity with contact angle measurements, J. Membr. Sci., 349 (2010) 349–357.
[33] Y.-N. Kwon, S.P. Hong, H.W. Choi, T.M. Tak, Surface modification of a polyamide reverse osmosis membrane for chlorine resistance improvement, J. Membr. Sci., 415–416 (2012) 192–198.
[34] A.E. Childress, M. Elimelech, Effect of solution chemistry on the surface charge of polymeric reverse osmosis and nanofiltration membranes, J. Membr. Sci., 119 (1996) 253–268.
[35] D. Saeki, T. Tanimoto, H. Matsuyama, Anti-biofouling of polyamide reverse osmosis membranes using phosphoryl-choline polymer grafted by surface-initiated atom transfer radical polymerization, Desalination, 350 (2014) 21–27.
[36] S. Davari, M. Omidkhah, M. Abdollahi, Improved antifouling ability of thin film composite polyamide membrane modified by a pH-sensitive imidazole-based zwitterionic polyelectrolyte, J. Membr. Sci., 564 (2018) 788–799.
[37] M.S. Rahaman, H. Thérien-Aubin, M. Ben-Sasson, C.K. Ober, M. Nielsen, M. Elimelech, Control of biofouling on reverse osmosis polyamide membranes modified with biocidal nanoparticles and antifouling polymer brushes, J. Mater. Chem. B, 2 (2014) 1724–1732.
[38] D.L. Shaffer, H. Jaramillo, S.R. Castrillón, X.L. Lu, M. Elimelech, Post-fabrication modification of forward osmosis membranes with a poly(ethylene glycol) block copolymer for improved organic fouling resistance, J. Membr. Sci., 490 (2015) 209–219.
[39] X.Y. Wei, Z. Wang, J. Xu, J.X. Wang, S.C. Wang, Surface modification of commercial aromatic polyamide reverse osmosis membranes by cross-linking treatments, Chin. J. Chem. Eng., 21 (2013) 473–484.
[40] Y. He, X.Y. Zhang, X.F. Zhang, H. Huang, J. Chang, H.Q. Chen, Structural investigations of toluene diisocyanate (TDI) and trimethylolpropane (TMP)-based polyurethane prepolymer, J. Ind. Eng. Chem., 18 (2012) 1620–1627.
[41] Z.L. Zhang, S. Wang, H.Y. Chen, Q.J. Liu, T. Wang, Preparation of polyamide membranes with improved chlorine resistance by bis-2,6-N,N-(2-hydroxyethyl) diaminotoluene and trimesoyl chloride, Desalination, 331 (2013) 16–25.
[42] S.S. Bing, J.Q. Wang, H. Xu, Y.Y. Zhao, Polyamide thin-film composite membrane modified with persulfate for improvement of perm-selectivity and chlorine-resistance, J. Membr. Sci., 555 (2018) 318–326.
[43] A. Tiraferri, Y. Kang, E.P. Giannelis, M. Elimelech, Superhydrophilic thin-film composite forward osmosis membranes for organic fouling control: fouling behavior and antifouling mechanisms, Environ. Sci. Technol., 46 (2012) 11135–11144.
[44] X.D. Weng, Y.L. Ji, R. Ma, F.Y. Zhao, Q.F. An, C.J. Gao, Superhydrophilic and antibacterial zwitterionic polyamide nanofiltration membranes for antibiotics separation, J. Membr. Sci., 510 (2016) 122–130.
[45] Y. Fan, H. Chen, Y. Lv, Z.H. Lv, S.C. Yu, M.H. Liu, Z.J. Gao, Improving the water permeability and antifouling property of thin-film composite polyamide nanofiltration membrane by modifying the active layer with the triethanolamine, J. Membr. Sci., 513 (2016) 108–116.
[46] J.M. Gohil, A.K. Suresh, A statistical study of the effect of preparation conditions on the structure and performance of thin film composite reverse osmosis membranes, Desal. Water Treat., 57 (2016) 2924–2941.
[47] A. Ettori, E. Gaudichet-Maurin, J.C. Schrotter, P. Aimar, C. Causser, Permeability and chemical analysis of aromatic polyamide based membranes exposed to sodium hypochlorite, J. Membr. Sci., 375 (2011) 220–230.
[48] S.J. Cao, G. Zhang, C. Xiong, S.R. Long, X.J. Wang, J. Yang, Preparation and characterization of thin-film-composite reverse-osmosis polyamide membrane with enhanced chlorine resistance by introducing thioether units into polyamide layer, J. Membr. Sci., 564 (2018) 473–482.
[49] V.T. Do, C.Y. Tang, M. Reinhard, J.O. Leckie, Degradation of polyamide nanofiltration and reverse osmosis membranes by hypochlorite, Environ. Sci. Technol., 46 (2012) 852–859.
[50] S. Gholami, A. Rezvani, V. Vatanpour, J.L. Cortina, Improving the chlorine resistance property of polyamide TFC RO membrane by polyethylene glycol diacrylate (PEGDA) coating, Desalination, 443 (2018) 245–255.